Inorganic Chemistry
Article

Inorg. Chem. **2010**, *49*, 5573–5583 **5573**
DOI: 10.1021/ic100494f

Basic Coordination Chemistry Relevant to DNA Adducts Formed by the Cisplatin Anticancer Drug. NMR Studies on Compounds with Sterically Crowded Chiral Ligands

Jamil S. Saad,*,†,§ Michele Benedetti,‡,∥ Giovanni Natile,‡ and Luigi G. Marzilli*,†

†*Departments of Chemistry, Louisiana State University, Baton Rouge, Louisiana 70803 and Emory University, Atlanta, Georgia 30322, and* ‡*Dipartimento Farmaco-Chimico, Università di Bari, Via E. Orabona, 4, 70125 bari, Italy.* §*Current address: Department of Microbiology, University of Alabama at Birmingham, 845 19th Street South, Birmingham, Alabama 35294.* ∥*Current address: Dipartimento di Scienze e Tecnologie Biologiche ed Ambientali, Università del Salento, Via Provinciale Lecce-Monteroni, 73100 Lecce, Italy.*

Received March 15, 2010

Me$_4$DAB Pt**G**$_2$ adducts with the bulky C_2-symmetric chiral diamine, **Me$_4$DAB** (*N*,*N*,*N*′,*N*′-tetramethyl-2,3-diaminobutane with *R*,*R* and *S*,*S* configurations at the chelate ring C atom, **G** = guanine derivative), exhibit slow conformer interchange and are amenable to characterization by NMR methods. The investigation of the *cis*-PtA_2**G**$_2$ adducts formed by clinically widely used anticancer drugs [A_2 = diaminocyclohexane, $(NH_3)_2$] is impeded by the rapid conformer interchange permitted by the low A_2 bulk near the inner coordination sphere. **Me$_4$DAB**Pt**G**$_2$ adducts exist as a mixture of exclusively head-to-tail (HT) conformers. No head-to-head (HH) conformer was observed. The **Me$_4$DAB** chirality significantly influences which HT chirality is favored (ΔHT for *S*,*S* and ΛHT for *R*,*R*). For simple **G** ligands, the ratio of favored HT conformer to less favored HT conformer is ∼2:1. For guanosine monophosphate (GMP) ligands, the phosphate group *cis* **G** N1H hydrogen bonding favors the ΛHT and the ΔHT conformers for 5′-GMP and 3′-GMP adducts, respectively. For both HT conformers of *cis*-PtA_2**G**$_2$ adducts, the **G** nucleobase plane normally cants with respect to the coordination plane in the same direction, left or right, for a given A_2 chirality. In contrast, the results for **Me$_4$DAB**Pt**G**$_2$ adducts provide the first examples of a change in the canting direction between the two HT conformers; this unusual behavior is attributed to the fact that canting always gives long **G** O6 to N−Me distances and that these **Me$_4$DAB** ligands have bulk both above and below the coordination plane. These results and ongoing preliminary studies of **Me$_4$DAB**Pt adducts with G residues linked by a phosphodiester backbone, which normally favors HH conformers, all indicate that a high percentage of HT conformer is present. Collectively, these findings advance fundamental concepts in Pt-DNA chemistry and may eventually help define the role of the carrier-ligand steric effects on anticancer activity.

Introduction

Platinum compounds of the type *cis*-PtX_2A_2 [X_2 = anionic leaving ligand(s), A_2 = one diamine or two amine carrier ligands] as well as other Pt compounds with trans ligands or with only one leaving ligand exhibit anticancer activity with cisplatin (*cis*-Pt$(NH_3)_2Cl_2$) and analogues, enjoying broad clinical usage for over a quarter of a century.[1−9] Pt(II) compounds target DNA and bind preferentially at the N7 atom of the guanine base (Figure 1). Cisplatin and the other widely used bifunctional drugs (including oxaliplatin), most frequently bind at the N7 atoms of adjacent G residues.[7,8,10−17]

*To whom correspondence should be addressed. Telephone: 205-996-9282 (J.S.S.), 225-578-0933 (L.G.M.). Fax: 205-996-4008 (J.S.S.), 225-578-3463 (L.G.M.). E-mail: saad@uab.edu (J.S.S.), lmarzil@lsu.edu (L.G.M.).

(1) Arnesano, F.; Natile, G. *Coord. Chem. Rev.* **2009**, *253*, 2070–2081.
(2) Centerwall, C. R.; Goodisman, J.; Kerwood, D. J.; Dabrowiak, J. C. *J. Am. Chem. Soc.* **2005**, *127*, 12768–12769.
(3) Decatris, M. P.; Sundar, S.; O'Byrne, K. J. *Cancer Treat. Rev.* **2004**, *30*, 53–81.
(4) Jakupec, M. A.; Galanski, M.; Arion, V. B.; Hartinger, C. G.; Keppler, B. K. *Dalton Trans.* **2008**, 183–194.
(5) Kelland, L. *Nat. Rev. Cancer* **2007**, *7*, 573–584.
(6) Klein, A. V.; Hambley, T. W. *Chem. Rev.* **2009**, *109*, 4911–4920.
(7) Lippert, B. *Cisplatin. Chemistry and Biochemistry of a Leading Anticancer Drug*; Wiley-VCH: Weinheim, Germany, 1999.
(8) Reedijk, J. *Eur. J. Inorg. Chem.* **2009**, *10*, 1303–1312.
(9) Wang, D.; Lippard, S. J. *Nat. Rev. Drug Discovery* **2005**, *4*, 307–320.
(10) Beljanski, V.; Villanueva, J. M.; Doetsch, P. W.; Natile, G.; Marzilli, L. G. *J. Am. Chem. Soc.* **2005**, *127*, 15833–15842.
(11) Chaney, S. G.; Campbell, S. L.; Temple, B.; Bassett, E.; Wu, Y.; Faldu, M. *J. Inorg. Biochem.* **2004**, *98*, 1551–1559.
(12) Natile, G.; Marzilli, L. G. *Coord. Chem. Rev.* **2006**, *250*, 1315–1331.
(13) Ober, M.; Lippard, S. J. *J. Am. Chem. Soc.* **2008**, *130*, 2851–2861.
(14) Ohndorf, U.-M.; Lippard, S. J. In *DNA damage recognition*; Siede, W., Kow, Y. W., Doetsch, P. W., Eds.; CRC: London, 2005; Vol. *12*, p 239−261.
(15) Bhattacharyya, D.; Marzilli, P. A.; Marzilli, L. G. *Inorg. Chem.* **2005**, *44*, 7644–7651.
(16) Kaspárková, J.; Vojtiskova, M.; Natile, G.; Brabec, V. *Chem.—Eur. J.* **2008**, *14*, 1330–1341.
(17) Malina, J.; Novakova, O.; Vojtiskova, M.; Natile, G.; Brabec, V. *Biophys. J.* **2007**, *93*, 3950–3962.

Published on Web 05/24/2010

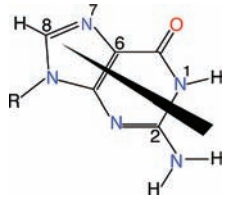

Figure 1. N9-guanine derivatives (the black triangle is used for a shorthand representation of the base with five- and six-membered rings at the triangle's tip and base, respectively). R is ethyl for 9-EtG, a sugar residue for nucleosides and a sugar−phosphate residue for nucleotides.

This intrastrand G*pG* cross-link lesion (G* = N7-platinated G residue) may trigger cell death, although the mechanism of action is not entirely understood. The search for a more active drug has prompted strong interest in the synthesis and screening of a large number of cisplatin analogues with carrier ligands varying in size and properties.[18,19] Although the decrease in activity of *cis*-PtA_2X_2 analogues across the series A = NH_3 > RNH_2 > R_2NH[18,20,21] could result from changes in biodistribution of the compound, the differences in the rate of reaction with DNA, or the differences in the interaction of the lesion with various recognition proteins, most interest has focused on the role of hydrogen bonding between the carrier ligand NH's and phosphate group oxygen atoms and/or G* O6 atoms. However, even in the case for which the N-donor has no NH groups, some anticancer activity has been detected.[22]

An X-ray/NMR-derived model of a duplex 9-oligomer[23] and an X-ray structure of an HMG-bound 16-oligomer,[24] both containing the intrastrand cisplatin lesion, and more recently an oligomer adduct of a rather bulky monofunctional Pt anticancer agent,[25,26] all have a similar unusual location of the base pair adjacent to the G* in the 5′-direction. These findings have suggested to us that, despite its small size, a ligand as small as ammonia may have large interligand interactions with this 5′-base pair of the DNA "ligand".[27] We believe that close interligand interactions result from the restraints imposed by the sugar−phosphate backbone. These restraints force clashes between ammonia and the base pair adjacent to the G*pG* cross-link when G*pG* exists in the usual head-to-head (HH) conformation (Figure 2). The restraints and resulting clashes might be so severe as to preclude the existence in DNA adducts of the less common head-to-tail (HT) conformation (Figure 2).[10,27,28]

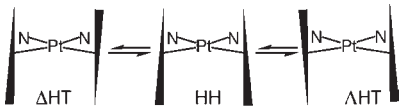

Figure 2. Shorthand representation of ΛHT, ΔHT, and HH conformations with the carrier ligand to the rear. (Black triangles with five- and six-membered rings at the triangle's tip and base, respectively.) For C_2-symmetric carrier ligands, the three conformers would give four sets of **G** NMR signals. The two HT conformers are C_2 symmetrical, and thus each gives one set of signals, whereas the HH conformer gives two sets of signals.

In contrast to the DNA duplex cross-link adducts, *cis*-PtA_2G_2 adducts lacking backbone restraints (boldface **G** = unlinked guanine derivative, Figure 1) highly favor the HT conformers over the HH conformer[29−35] with very few exceptions.[36,37] Interconversions between HH and HT conformations via rotation about the Pt−**G** N7 bonds in *cis*-PtA_2G_2 and cross-link adducts[12,31,38−41] are rapid on the NMR time scale, and bulky carrier ligands are needed to lower the rate to allow observation of NMR signals of the conformers present in solution.[27,29,30,32−38,42] The pioneering study in this field used *N*,*N*,*N*′,*N*′-tetramethylethylenediamine (**Me$_4$EN**).[31] (Bidentate carrier ligands are designated with boldface type.) **Me$_4$EN**Pt**G**$_2$ adducts were shown to exist as HT conformers in the solid state and in solution.[20,31] For **Me$_4$EN**Pt**G**$_2$ adducts in solution, no HH conformer was reported, and the Δ or Λ chirality of the HT conformer (Figure 2) could not be determined.[43]

We discovered that the HH conformer existed in adducts with the two related C_2-symmetric carrier ligands, **Me$_2$DAB** (*N*,*N*′-dimethyl-2,3-diaminobutane) and **Bip** (2,2′-bipiperidine) (Figure 3).[12,29,30,33−36,44] The **Me$_2$DAB**Pt and **Bip**Pt moieties have *S*,*R*,*R*,*S* and *R*,*S*,*S*,*R* enantiomeric configurations, in which the chiral centers point to the N, C, C, and N chelate ring atoms, respectively (Figure 3). The relative size of NOE cross-peaks between the chiral carrier

(18) Hambley, T. W. *Coord. Chem. Rev.* **1997**, *166*, 181–223.
(19) Haxton, K. J.; Burt, H. M. *J. Pharm. Sci.* **2009**, *98*, 2299–2316.
(20) Orbell, J. D.; Taylor, M. R.; Birch, S. L.; Lawton, S. E.; Vilkins, L. M.; Keefe, L. J. *Inorg. Chim. Acta* **1988**, *152*, 125–134.
(21) Benedetti, M.; Malina, J.; Kaspárková, J.; Brabec, V.; Natile, G. *Environ. Health Perspect.* **2002**, *110*, 779–782.
(22) Milanesio, M.; Monti, E.; Gariboldi, M. B.; Gabano, E.; Ravera, M.; Osella, D. *Inorg. Chim. Acta* **2008**, *361*, 2803–2814.
(23) Marzilli, L. G.; Saad, J. S.; Kuklenyik, Z.; Keating, K. A.; Xu, Y. *J. Am. Chem. Soc.* **2001**, *123*, 2764–2770.
(24) Ohndorf, U.-M.; Rould, M. A.; He, Q.; Pabo, C. O.; Lippard, S. J. *Nature* **1999**, *399*, 708–712.
(25) Lovejoy, K. S.; Todd, R. C.; Zhang, S.; McCormick, M. S.; D'Aquino, J. A.; Reardon, J. T.; Sancar, A.; Giacomini, K. M.; Lippard, S. J. *Proc. Natl. Acad. Sci. U.S.A.* **2008**, *105*, 8902–8907.
(26) Todd, R. C.; Lippard, S. J. In *Platinum and Other Heavy Metal Compounds in Cancer Chemotherapy*; Bonetti, A., Leone, R., Muggia, F. M., Howell, S. B., Eds.; Humana Press: New York, 2009, p 67−72.
(27) Saad, J. S.; Natile, G.; Marzilli, L. G. *J. Am. Chem. Soc.* **2009**, *131*, 12314–12324.
(28) Sullivan, S. T.; Saad, J. S.; Fanizzi, F. P.; Marzilli, L. G. *J. Am. Chem. Soc.* **2002**, *124*, 1558–1559.
(29) Ano, S. O.; Intini, F. P.; Natile, G.; Marzilli, L. G. *J. Am. Chem. Soc.* **1997**, *119*, 8570–8571.
(30) Ano, S. O.; Intini, F. P.; Natile, G.; Marzilli, L. G. *Inorg. Chem.* **1999**, *38*, 2989–2999.
(31) Cramer, R. E.; Dahlstrom, P. L. *J. Am. Chem. Soc.* **1979**, *101*, 3679–3681.
(32) Kiser, D.; Intini, F. P.; Xu, Y.; Natile, G.; Marzilli, L. G. *Inorg. Chem.* **1994**, *33*, 4149–4158.
(33) Marzilli, L. G.; Intini, F. P.; Kiser, D.; Wong, H. C.; Ano, S. O.; Marzilli, P. A.; Natile, G. *Inorg. Chem.* **1998**, *37*, 6898–6905.
(34) Saad, J. S.; Scarcia, T.; Natile, G.; Marzilli, L. G. *Inorg. Chem.* **2002**, *41*, 4923–4935.
(35) Xu, Y.; Natile, G.; Intini, F. P.; Marzilli, L. G. *J. Am. Chem. Soc.* **1990**, *112*, 8177–8179.
(36) Saad, J. S.; Scarcia, T.; Shinozuka, K.; Natile, G.; Marzilli, L. G. *Inorg. Chem.* **2002**, *41*, 546–557.
(37) Sullivan, S. T.; Ciccarese, A.; Fanizzi, F. P.; Marzilli, L. G. *Inorg. Chem.* **2001**, *40*, 455–462.
(38) Ano, S. O.; Kuklenyik, Z.; Marzilli, L. G. In *Cisplatin. Chemistry and Biochemistry of a Leading Anticancer Drug*; Lippert, B., Ed.; Wiley-VCH: Weinheim, Germany, 1999, p 247−291.
(39) Ano, S. O.; Intini, F. P.; Natile, G.; Marzilli, L. G. *J. Am. Chem. Soc.* **1998**, *120*, 12017–12022.
(40) Williams, K. M.; Cerasino, L.; Natile, G.; Marzilli, L. G. *J. Am. Chem. Soc.* **2000**, *122*, 8021–8030.
(41) Sullivan, S. T.; Ciccarese, A.; Fanizzi, F. P.; Marzilli, L. G. *J. Am. Chem. Soc.* **2001**, *123*, 9345–9355.
(42) Sullivan, S. T.; Ciccarese, A.; Fanizzi, F. P.; Marzilli, L. G. *Inorg. Chem.* **2000**, *39*, 836–842.
(43) Cramer, R.; Dahlstrom, P. *Inorg. Chem.* **1985**, *24*, 3420–3424.
(44) Marzilli, L. G.; Ano, S. O.; Intini, F. P.; Natile, G. *J. Am. Chem. Soc.* **1999**, *121*, 9133–9142.

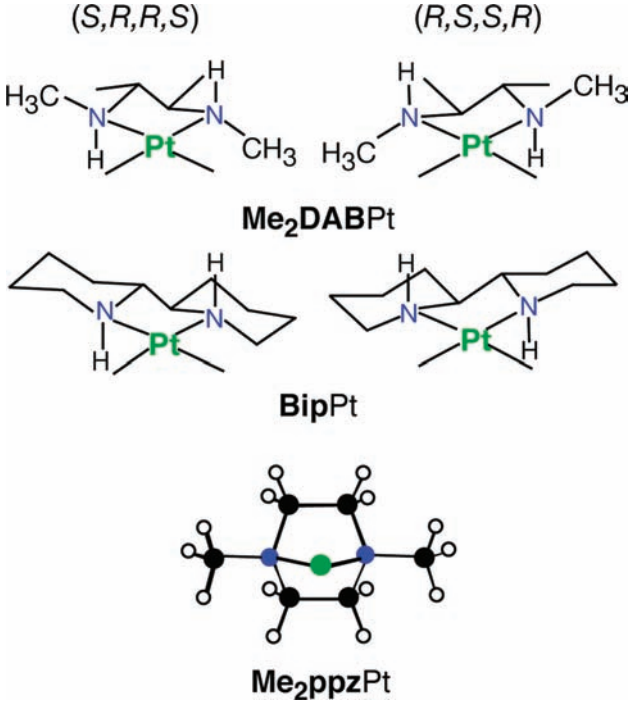

Figure 3. Sketches of the **Bip**Pt and **Me$_2$DAB**Pt moieties with *S*,*R*,*R*,*S* or *R*,*S*,*S*,*R* chirality (stereochemistry defined for the N, C, C, and N ring atoms of the carrier-ligand backbone) and ball-and-stick figure of **Me$_2$ppz**Pt.

ligand and **G** H8 signals allowed us to determine the Δ and Λ chirality of the HT conformers.

As mentioned, structure−activity relationships implicate the **G** O6 to NH hydrogen bond (H-bond) as possibly relevant to anticancer activity. Such H-bonds were found in many examples of adducts with carrier ligands having N-donors with at least one hydrogen (e.g., NH_3, RNH_2, and R_2NH).[12] However, because the strong Pt−N7 bond forces the juxtaposition of the **G** O6 and NH atoms in such cases, the strength of such an H-bond cannot be assessed. In contrast, for the HT conformers of the *cis*-PtA_2**G**$_2$ adducts with the **Me$_2$DAB** and **Bip** carrier ligands, only one HT conformer could form the **G** O6 to NH H-bond.[12] This conformer invariably proved to be less stable than the other HT conformer, which could not form such H-bonds.[12] This result contradicted the paradigm of the day. We now believe that water forms stronger H-bonds to the NH than does **G** O6.[41] The O6 of one **G** of the HH conformer of these same adducts is forced to be relatively close to an NH. The plane of this **G** nucleobase is canted with respect to the Pt coordination in the direction allowing the **G** O6 to NH H-bond to form. However, this H-bonding does not necessarily stabilize the HH conformer because the HH conformer was observed for adducts of the type, **Me$_2$ppz**Pt**G**$_2$ (**Me$_2$ppz** = *N*,*N*′-dimethylpiperazine, Figure 3).[37,42] These first reports of an HH conformer for a *cis*-PtA_2**G**$_2$ model in which the A_2 ligand lacks an NH group establish that an NH group is not needed for an HH conformation to exist, at least when there is no out-of-plane bulk. Subsequent studies confirmed this conclusion.[45,46]

(45) Maheshwari, V.; Bhattacharyya, D.; Fronczek, F. R.; Marzilli, P. A.; Marzilli, L. G. *Inorg. Chem.* **2006**, *45*, 7182–7190.
(46) Maheshwari, V.; Marzilli, P. A.; Marzilli, L. G. *Inorg. Chem.* **2008**, *47*, 9303–9313.

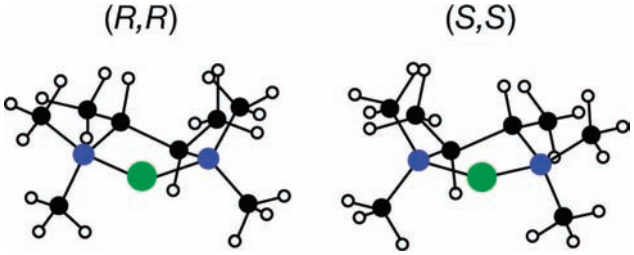

Figure 4. Ball-and-stick figures of the **Me$_4$DAB**Pt moieties with *S*,*S* or *R*,*R* chirality (stereochemistry defined for the carbon ring atoms of the carrier-ligand backbone).

As part of our efforts to understand the influence of out-of-plane bulk on conformer stability and properties, we now employ **Me$_4$DAB**Pt**G**$_2$ adducts [**Me$_4$DAB** = *N*,*N*,*N*′,*N*′-tetramethyl-2,3-diaminobutane, Figure 4; **G** = 5′-GMP, 3′-GMP, Guo (guanosine), 1-MeGuo (1-methylguanosine), and 9-EtG (9-ethylguanine)]. The **Me$_4$DAB** ligand has two C_2-symmetrical geometries, with *S*,*S* or *R*,*R* configurations at the asymmetric C atoms of the chelate ring (Figure 4). The chirality allows us to use NMR methods to establish the absolute conformation of the HT conformers. A major goal of this work was to use these close analogues of **Me$_4$EN** to understand why the classic study[31] employing this ligand did not reveal the presence of an HH conformer. One hypothesis is that the HH conformer was not observed because that study did not include the 5′-GMP ligand, the **G** ligand normally giving the most HH conformer.[29,30,33−36] A second hypothesis is that the presence at any given time of two quasi-axial N-Me groups in the **Me$_4$EN** ligand makes the HH conformer unstable. Compared to the **Me$_2$DAB**Pt(5′-GMP)$_2$ adducts with the symmetrical **Me$_2$DAB** ligands, in which both N-Me groups are quasi-equatorial, (*S*,*R*,*R*,*R*)- and (*R*,*S*,*S*,*S*)-**Me$_2$DAB**Pt(5′-GMP)$_2$ adducts had very low populations of the HH conformer.[32] In these carrier ligands, one N-Me is quasi-equatorial, and one is quasi-axial. Thus, the study of 5′-GMP adducts had special relevance in the current study. Finally, in the Discussion Section, we introduce and assess other types of interligand interactions as well as other structural features, such as base canting.

Our studies employing chiral diamines are directly relevant to the Pt anticancer field. For example, **Me$_4$EN**PtCl_2 has been tested for cytotoxic effects on human ovarian carcinoma cells in parallel studies with cisplatin.[22] Furthermore, the elucidation of interligand interactions has fundamental relevance to many fields, such as asymmetric catalysis.

Experimental Section

Synthesis of Me$_4$DABPt(NO$_3$)$_2$ Complexes. A detailed procedure for synthesizing **Me$_4$DAB**Pt$(NO_3)_2$ complexes is described in Supporting Information. The purity of (*S*,*S*)- and (*R*,*R*)-**Me$_4$DAB**Pt$(NO_3)_2$ complexes was confirmed by ^{1}H NMR spectroscopy (Supporting Information).

Materials and Sample Preparation. 5′-GMP, 3′-GMP, Guo, 1-MeGuo, and 9-EtG were used as received from Sigma. A typical preparation involved treatment of ∼2 equiv of **G** with 1 equiv (∼5 mM) of **Me$_4$DAB**Pt$(NO_3)_2$ in D_2O (0.6 mL) at pH ∼4; reactions were conducted at 50−60 °C. Reactions were monitored by ^{1}H NMR spectroscopy until either no free **G** H8 signal or no change in H8 signal intensity was observed. Stock solutions of DNO_3, NaOD, and DCl (in D_2O) were used for adjusting the pH of the samples directly in the NMR tubes when needed. When the pH was high (7 or 10), samples were dissolved

in 90% H_2O/10% D_2O to avoid H/D exchange. These samples were heated at ~60 °C for 2 days to ensure attainment of equilibrium.

NMR Spectroscopy. NMR spectra were obtained on a Varian (Unity or Inova) 600 MHz and Bruker Avance II (700 MHz ^{1}H) spectrometer equipped with a cryoprobe, processed with Felix or NMRPIPE,[47] and analyzed with NMRVIEW.[48] The two-dimensional (2D) phase-sensitive NOESY spectra were performed at 5 °C and pH ~4 (mixing time = 1000 ms). The decoupled ^{1}H−^{13}C heteronuclear multiple quantum coherence (HMQC) data were collected at 25 °C. For ^{195}Pt NMR spectroscopy, the [*rac*-**Me$_4$DAB**Pt(9-EtG)$_2$]$^{2+}$ NMR sample was prepared as described above but at ~20 mM Pt. The ^{195}Pt NMR spectra were collected on a Varian Unity 600 MHz instrument operating at 128.6 MHz (Na_2PtCl_6 external reference). Relative percentages of conformers were calculated by using **G** H8 or N-Me signals of the **Me$_4$DAB** ligand when the H8 signals overlapped.

CD Spectroscopy. CD samples of ~5×10^{-5} M **G** were prepared by diluting aliquots from the NMR samples. Spectra were collected (λ = 200−350 nm) on a JASCO 600 spectropolarimeter at room temperature. Four scans recorded in succession were averaged to improve the signal/noise ratio. After the pH was changed, CD samples were kept at ~60 °C for 2 days to reach equilibrium.

Results

Formation Reactions. The magnetically equivalent halves of the C_2-symmetric **Me$_4$DAB**Pt moiety of [(*R*,*R*)- or (*S*,*S*)-**Me$_4$DAB**Pt(D$_2$O)$_2$]$^{2+}$ (pH ~4) had the expected NMR signals (a broad CH multiplet at 3.20 ppm, two N-Me singlets at 2.73 and 2.76 ppm, and a C-Me doublet at 1.08 ppm) (Supporting Information). On treatment of either [**Me$_4$DAB**Pt(D$_2$O)$_2$]$^{2+}$ cation with a **G** derivative, the initial ^{1}H NMR spectra contained signals of transient as well as final species. For **Me$_4$DAB**Pt**G**$_2$ adducts, four **G** H8 ^{1}H NMR signals (one for each HT conformer and two signals of equal intensity for the HH conformer, Figure 2) are possible when **G** contained a sugar residue. However, only two persistent **G** H8 signals were observed, and these were assigned to the HT conformers for a number of reasons. When the pH was lowered to ~1, the new **G** H8 signals did not shift, indicating that Pt was bound to **G** N7. The **G** H8 signals (downfield from the free **G** H8 signal) of the two final products have different intensities, consistent with formation of the two HT conformers (cf. Figure 2). Also, the fact that the 2D NOESY data show no H8−H8 cross-peak rules out a HH conformer. Equilibrium between the two HT conformers was reached after ~24 h (at 60 °C).

Assignment of Absolute Conformation. Normally we determine the absolute conformation (ΛHT and ΔHT) of HT conformers by assessing NOE cross-peaks to a chiral carrier ligand of known absolute configuration.[33] Details on signal assignments are described in Supporting Information. Furthermore, enhanced CD signals observed previously for *cis*-Pt**A**$_2$**G**$_2$ adducts were utilized to identify the dominant conformer in solution.[30,33,34,36,37,42,49−51] The similarity of the CD features of a particular HT conformer for all previously studied *cis*-Pt**A**$_2$**G**$_2$ adducts[12,30,33,34,36,37,42,49−53] led us to conclude that the CD features reflect the dominant HT conformer in solution regardless of the identity of the carrier ligand. For almost all **Me$_4$DAB**Pt**G**$_2$ adducts, the CD signal was relatively strong, and the features have now well-established characteristics: a positive feature at ~280 nm and negative features at ~250 and ~210 nm for the ΛHT conformer and the opposite signs at these wavelengths for the ΔHT conformer.[12,30,33,34,36,37,42,49−53]

The ΔHT conformer was initially more favored (~30 min) for (*R*,*R*)-**Me$_4$DAB**Pt(5′-GMP)$_2$, (*S*,*S*)-**Me$_4$DAB**Pt(5′-GMP)$_2$, and (*R*,*R*)-**Me$_4$DAB**Pt(3′-GMP)$_2$ (Supporting Information). With time, the ΛHT conformer increased in abundance; after equilibrium was reached, the ΛHT conformer was clearly dominant for (*R*,*R*)-**Me$_4$DAB**Pt(5′-GMP)$_2$ and (*R*,*R*)-**Me$_4$DAB**Pt(3′-GMP)$_2$ and only slightly favored for (*S*,*S*)-**Me$_4$DAB**Pt(5′-GMP)$_2$. For (*S*,*S*)-**Me$_4$DAB**Pt(3′-GMP)$_2$, the HT conformers formed in similar amounts; the ΔHT conformer became dominant after equilibrium was reached (Supporting Information). These results are very similar to those observed for **Me$_4$DACH**Pt**G**$_2$ adducts (**Me$_4$DACH** = *N*,*N*,*N*′,*N*′-tetramethyl-1,2-diaminocyclohexane).[53] Our data indicate that the **Me$_4$DAB** ligand greatly reduced the rate of **G** base rotation. Likewise, for **Me$_2$ppz**Pt**G**$_2$ and **Bip**Pt**G**$_2$ adducts, **G** base rotation was very slow.[29,30,37,42] For **Bip**Pt**G**$_2$ adducts, conformer distribution reached equilibrium in ~2−4 h after varying the pH. In contrast, EXSY cross-peaks were observed for **Me$_2$DAB**Pt(5′-GMP)$_2$ and **Me$_2$DAB**Pt(1-Me-5′-GMP)$_2$ at 5 °C.[33,36] These adducts equilibrate rapidly. Because the pH studies of **Me$_4$DAB**Pt**G**$_2$ complexes showed that equilibrium can be reached after ~2 days only when samples were heated at ~60 °C, we conclude that the **Me$_4$DAB** ligand hinders **G** base rotation more effectively than do the **Bip**, **Me$_2$ppz**, and **Me$_2$DAB** ligands.

(*R*,*R*)-Me$_4$DABPt(5′-GMP)$_2$. The **G** H8 signals of the HT forms of (*R*,*R*)-**Me$_4$DAB**Pt(5′-GMP)$_2$ partially overlapped (pH of 4.1, Figure 5). As the pH was increased from 4.1 to 7.3, the HT H8 signals shifted upfield (Table 1); after ~2 days at 60 °C, the abundance of the major HT conformer increased slightly (Figure 5 and Table 2). Increasing the pH from 7.3 to 10.4 caused only small changes in the shifts of the H8 signals but the abundance of the conformers changed significantly (Table 2). The 2D NOESY data collected at pH 4.1 (Figure 5) revealed that ΛHT is the abundant conformer.

The CD spectrum of (*R*,*R*)-**Me$_4$DAB**Pt(5′-GMP)$_2$ at pH 4.1 exhibited the ΛHT shape (positive feature at ~280 nm and negative features at ~250 and ~210 nm, Figure 6). When the pH was raised from 4.1 to 7.3 and the sample held at pH 7.3 for 2 days at 60 °C, an increase in the intensities of the positive and negative CD features was observed (Figure 6). Upon increasing the pH from 7.3 to 10.4, the CD spectrum changed immediately, owing to N1H deprotonation. After 2 days at pH 10.4 and 60 °C,

(47) Delaglio, F.; Grzesiek, S.; Vuister, G. W.; Zhu, G.; Pfeifer, J.; Bax, A. *J. Biomol. NMR* **1995**, *6*, 277–293.
(48) Johnson, B. A.; Blevins, R. A. *J. Biomol. NMR* **1994**, *4*, 603–614.
(49) Wong, H. C.; Coogan, R.; Intini, F. P.; Natile, G.; Marzilli, L. G. *Inorg. Chem.* **1999**, *38*, 777–787.
(50) Wong, H. C.; Intini, F. P.; Natile, G.; Marzilli, L. G. *Inorg. Chem.* **1999**, *38*, 1006–1014.
(51) Wong, H. C.; Shinozuka, K.; Natile, G.; Marzilli, L. G. *Inorg. Chim. Acta* **2000**, *297*, 36–46.
(52) Benedetti, M.; Marzilli, L. G.; Natile, G. *Chem.—Eur. J.* **2005**, *11*, 5302–5310.
(53) Benedetti, M.; Saad, J. S.; Marzilli, L. G.; Natile, G. *J. Chem. Soc., Dalton Trans.* **2003**, 872–879.

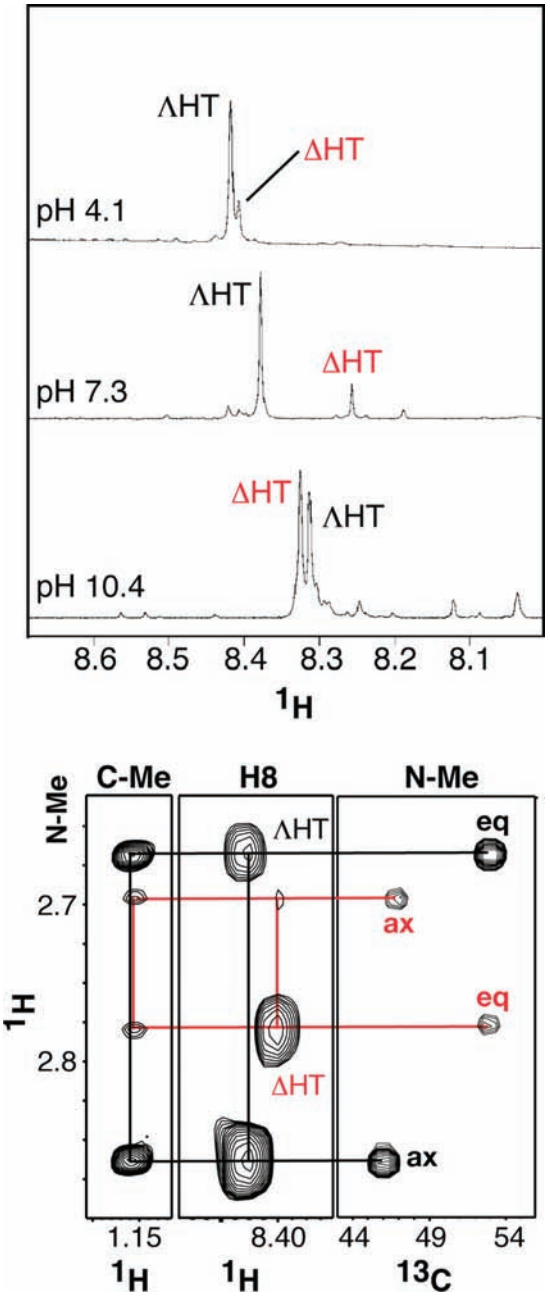

Figure 5. Representative NMR data collected for (*R*,*R*)-**Me$_4$DAB**Pt-(5′-GMP)$_2$. (Top) H8 ^{1}H NMR signals at different pH values (23 °C). (Bottom) Selected regions of the 2D NOESY and HMQC spectra at pH 4.0 (all scales are in ppm).

the intensities of both the positive and negative features decreased, indicating a roughly equal abundance of the HT conformers at pH 10.4.[30,33,34,36,49,50] Collectively, the NMR and CD data demonstrate that the ΛHT conformer dominates at pH 4.1 and 7.3 but not at pH 10.4.

(*S*,*S*)-Me$_4$DABPt(5′-GMP)$_2$. The NMR data revealed that the ΛHT conformer of (*S*,*S*)-**Me$_4$DAB**Pt(5′-GMP)$_2$ (pH 4.0) was slightly more abundant than the ΔHT conformer, which became even more favored at pH 7.4 (Figure 7). At pH ∼10, the ΔHT conformer became highly dominant. The CD spectra of (*S*,*S*)-**Me$_4$DAB**Pt(5′-GMP)$_2$ at pH 4.0 and 7.4 indicate that the abundant conformer has the ΛHT conformation (Supporting Information). At pH 10.3, where the **G** N1H is deprotonated, the CD features

Table 1. G H8 Shifts as a Function of pH for **Me$_4$DAB**Pt**G**$_2$ Complexes

		(*R*,*R*)			(*S*,*S*)		
G	conformer	pH ∼4	pH ∼7	pH ∼10	pH ∼4	pH ∼7	pH ∼10
5′-GMP	ΛHT	8.42	8.38	8.31	8.43	8.36	8.32
	ΔHT	8.41	8.26	8.33	8.41	8.28	8.34
3′-GMP	ΛHT	8.45	8.45	8.38	8.45	8.45	8.41
	ΔHT	8.51	8.60	8.34	8.54	8.66	8.33
Guo	ΛHT	8.44	8.44	–	8.43	8.43	–
	ΔHT	8.44	8.44	–	8.46	8.46	–
1-MeGuo	ΛHT	8.42	–	–	8.41	–	–
	ΔHT	8.41	–	–	8.44	–	–
9-EtG[a]	ΛHT	8.22	8.22	8.05	8.21	8.21	8.04
	ΔHT	8.21	8.21	8.04	8.22	8.22	8.05

[a] See text.

Table 2. Conformer Percentage as a Function of pH for **Me$_4$DAB**Pt**G**$_2$ Complexes

		(*R*,*R*)			(*S*,*S*)		
G	conformer	pH ∼4	pH ∼7	pH ∼10	pH ∼4	pH ∼7	pH ∼10
5′-GMP	ΛHT	77	86	45	56	61	21
	ΔHT	23	14	55	44	39	80
3′-GMP	ΛHT	67	48	80	36	21	47
	ΔHT	33	52	20	64	79	53
Guo	ΛHT	63	63	–	37	37	–
	ΔHT	37	37	–	63	63	–
1-MeGuo	ΛHT	65	–	–	35	–	–
	ΔHT	35	–	–	65	–	–
9-EtG[a]	ΛHT	63	63	63	37	37	37
	ΔHT	37	37	37	63	63	63

[a] See text.

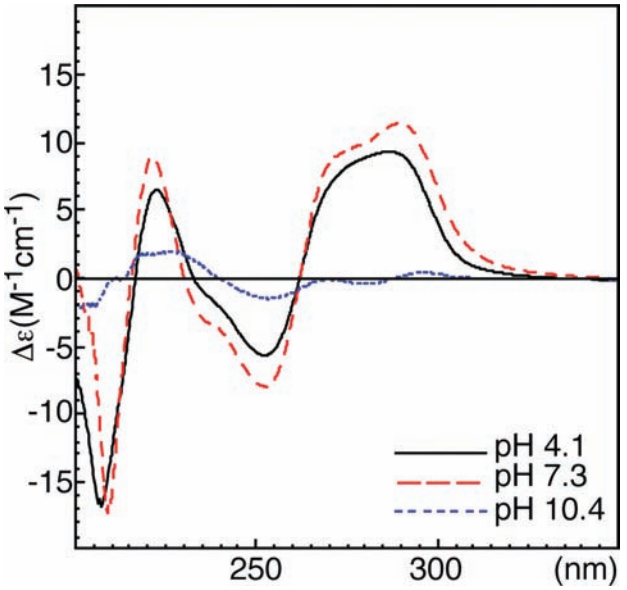

Figure 6. CD spectra of (*R*,*R*)-**Me$_4$DAB**Pt(5′-GMP)$_2$ at different pH values.

are inverted, an indication of the ΔHT conformation, as found by NMR spectroscopy.

(*R*,*R*)-Me$_4$DABPt(3′-GMP)$_2$. The NMR (cf. Figure 8) and CD data (Supporting Information) are consistent with the ΛHT conformer being favored at pH 4.1. At pH 7.4, the ΔHT conformer increased in abundance and became slightly more favored. At pH 10.3, the ΛHT conformer became highly dominant (Figure 8 and Table 2).

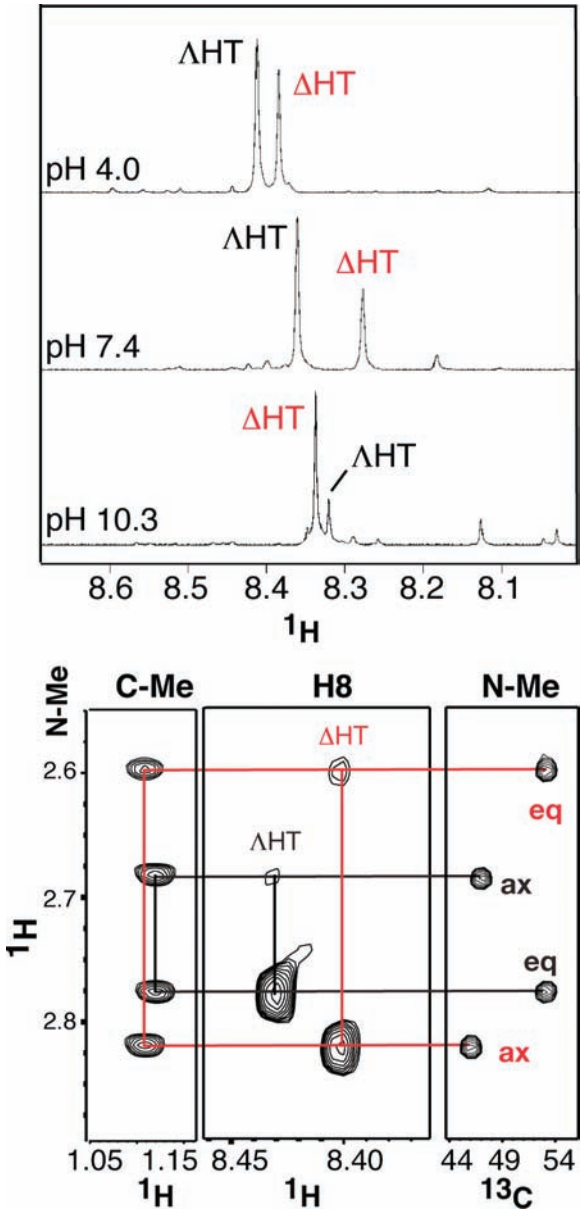

Figure 7. Representative NMR data collected for (*S*,*S*)-**Me$_4$DAB**Pt(5′-GMP)$_2$. (Top) H8 ^{1}H NMR signals collected at different pH values (23 °C). (Bottom) Selected regions of the 2D NOESY and HMQC spectra at pH 4.0 (all scales are in ppm).

(*S*,*S*)-Me$_4$DABPt(3′-GMP)$_2$. The H8 shifts and distribution for the (*S*,*S*)-**Me$_4$DAB**Pt(3′-GMP)$_2$ HT forms were dependent on the pH (Figure 9; Tables 1 and 2). The major ΔHT conformer at pH 4.0 became highly dominant at pH 7.4 but was only slightly favored at pH 10.3. At pH 4.1 and 7.4, the CD spectra of (*S*,*S*)-**Me$_4$DAB**Pt(3′-GMP)$_2$ indicate that the most abundant conformer has the ΔHT conformation (Figure 10).[30,33,34,36,42] At pH 10.3, the CD spectrum had weak features but was still characteristic of the ΔHT conformation, a result consistent with the NMR data.

[(*R*,*R*)-Me$_4$DABPt(Guo)$_2$]$^{2+}$. For [(*R*,*R*)-**Me$_4$DAB**Pt(Guo)$_2$]$^{2+}$, two H8 signals in a 2:1 ratio at pH 4.2 and 7.0 were assigned to the two HT conformers (Supporting Information). The CD spectrum of [(*R*,*R*)-**Me$_4$DAB**Pt(Guo)$_2$]$^{2+}$ at pH 4.0 indicates a dominant ΛHT conformer (Supporting Information).[30,33,34,36,42]

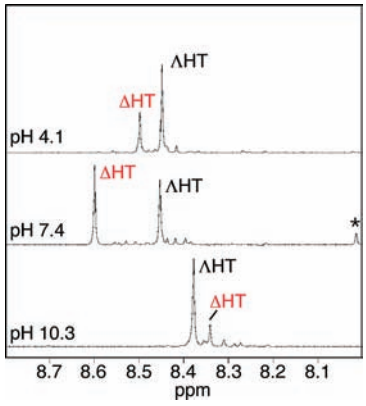

Figure 8. H8 ^{1}H NMR signals of (*R*,*R*)-**Me$_4$DAB**Pt(3′-GMP)$_2$ at different pH values (23 °C). Asterisk marks the signal for free 3′-GMP.

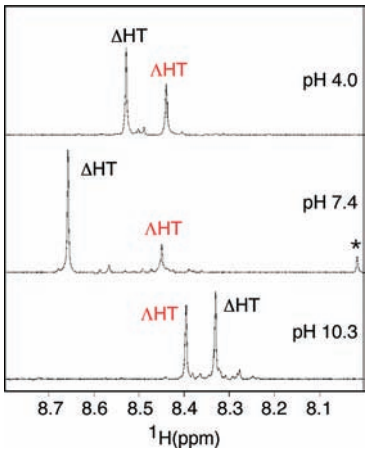

Figure 9. H8 ^{1}H NMR signals of (*S*,*S*)-**Me$_4$DAB**Pt(3′-GMP)$_2$ at different pH values (23 °C). Asterisk marks the signal for free 3′-GMP.

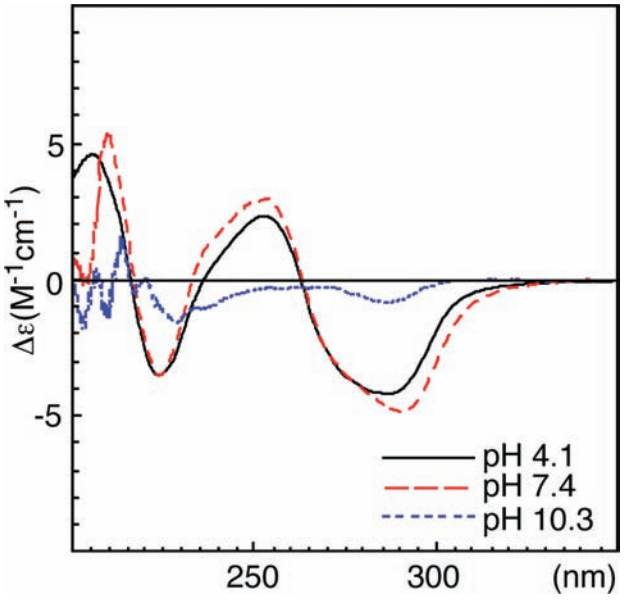

Figure 10. CD spectra of (*S*,*S*)-**Me$_4$DAB**Pt(3′-GMP)$_2$ at different pH values.

[(*S*,*S*)-Me$_4$DABPt(Guo)$_2$]$^{2+}$. The two HT conformers observed for [(*S*,*S*)-**Me$_4$DAB**Pt(Guo)$_2$]$^{2+}$ had a 2:1 ratio at pH 4.0 and 7.0 (Supporting Information). The CD

spectrum of [(*S*,*S*)-**Me$_4$DAB**Pt(Guo)$_2$]$^{2+}$ at pH 4.0 (Supporting Information) indicates a ΔHT conformation for the dominant form.[30,33,34,36,42]

[(*R*,*R*)-Me$_4$DABPt(1-MeGuo)$_2$]$^{2+}$ and [(*S*,*S*)-Me$_4$DABPt-(1-MeGuo)$_2$]$^{2+}$. Two H8 signals were found for each [**Me$_4$-DAB**Pt(1-MeGuo)$_2$]$^{2+}$ adduct (Supporting Information). At pH 4.1, the relative percentages for the two HT forms were similar to those observed for the Guo analogue (Table 2). No changes in H8 shifts or relative intensity were observed as a function of pH. The CD features, characteristic of the ΛHT conformer for [(*R*,*R*)-**Me$_4$DAB**Pt(1-MeGuo)$_2$]$^{2+}$ and the ΔHT conformer for [(*S*,*S*)-**Me$_4$DAB**Pt(1-MeGuo)$_2$]$^{2+}$ (data not shown), did not change as a function of pH.

[*rac*-Me$_4$DABPt(9-EtG)$_2$]$^{2+}$. For [*rac*-**Me$_4$DAB**Pt(9-EtG)$_2$]$^{2+}$, without the sugar moiety, two pairs of true HT enantiomers must be present. Because the members of each pair have equivalent signals, two H8 signals were observed (Table 2 and Supporting Information). At equilibrium at pH 7.0, the HTa signal is about half as large as the HTb signal. The assignment of these signals to the two pairs, the ΔHT [(*R*,*R*)-**Me$_4$DAB**Pt(9-EtG)$_2$]$^{2+}$ and ΛHT [(*S*,*S*)-**Me$_4$DAB**Pt(9-EtG)$_2$]$^{2+}$ pair and the ΛHT [(*R*,*R*)-**Me$_4$DAB**Pt(9-EtG)$_2$]$^{2+}$ and ΔHT [(*S*,*S*)-**Me$_4$DAB**Pt-(9-EtG)$_2$]$^{2+}$ pair, is described in the Discussion. At pH 10.0, the HT signals shifted by 0.15 ppm but no change in distribution occurred (Tables 1 and 2).

^{1}H−^{13}C HMQC NMR Data. We have obtained ^{1}H−^{13}C HMQC NMR data for all (*R*,*R*)- and (*S*,*S*)-**Me$_4$DAB**Pt**G**$_2$ adducts with **G** = 5′-GMP and 3′-GMP as well as [*rac*-**Me$_4$DAB**Pt(9-EtG)$_2$]$^{2+}$. Regardless of the nature of the carrier ligand or the **G** base, the C8 chemical shifts for HT conformers were almost identical (∼142−142.5 ppm). These C8 shifts are also similar to that observed for the *cis*-Pt(NH$_3$)$_2$(5′-GMP)$_2$ complex (143 ppm, data not shown). Interestingly, a pattern has been observed for the carrier−ligand N-Me ^{13}C NMR signals. Each HT conformer had two N-Me ^{13}C NMR signals at ∼53.0 and ∼46.0 ppm (Figures 5 and 7; Supporting Information, S3 and S5). The N-Me group that is anti to the CH group (CH$_3$−N−C−H torsion angle = ∼160−180°) is upfield (∼46 ppm), while the second N-Me group, in a position gauche to the CH group (CH$_3$−N−C−H torsion angle = ∼50−90°), is downfield (∼53 ppm). The significant difference in the ^{13}C NMR shifts of the HT N-Me groups is probably a result of the axial/equatorial nature of these groups or is caused by the proximity of the C-Me group. The ^{13}C NMR shifts of the equatorial substituents were found to be ∼3−6 ppm more downfield than the axial substituents for cyclohexane derivatives.[54]

^{195}Pt NMR Results. ^{195}Pt NMR signal shifts are sensitive parameters that have often been used to identify the number, type, and geometrical arrangement of coordinated ligands. Although one ^{195}Pt NMR signal was reported for *cis*-Pt(NH$_3$)$_2$(5′-GMP)$_2$ and [**EN**Pt(Guo)$_2$]$^{2+}$ (**EN** = ethylenediamine) complexes at −2455 and −2662 ppm, respectively,[55] separate ^{195}Pt NMR signals for the HH and HT conformers were observed for **Me$_2$ppz**Pt**G**$_2$ adducts.[37] For [*rac*-**Me$_4$DAB**Pt(9-EtG)$_2$]$^{2+}$, a broad ^{195}Pt NMR signal at −2492 ppm (pH ∼7, data not shown) was observed, indicating an overlap of HTa and HTb signals. In comparison, the ^{195}Pt NMR signals for the HT and HH conformers of **Me$_2$ppz**Pt(5′-GMP)$_2$ were observed at −2480 and −2471 ppm, respectively.[37] Thus, the ^{195}Pt NMR shifts for the HT conformers of **Me$_2$ppz**Pt(GMP)$_2$ and [*rac*-**Me$_4$DAB**Pt(9-EtG)$_2$]$^{2+}$ are similar.

Discussion

Assignments of Conformers. In other nondynamic *cis*-Pt**A**$_2$**G**$_2$ adducts (**Me$_2$DAB**Pt**G**$_2$, **Bip**Pt**G**$_2$, and **Me$_2$ppz**-Pt**G**$_2$),[29,30,33−37,42] the HH conformer was always present, with two equally intense H8 signals connected by a NOESY cross-peak. As revealed by the 2D NOESY spectra of (*R*,*R*)- and (*S*,*S*)-**Me$_4$DAB**Pt**G**$_2$ adducts with **G** = 5′-GMP and 3′-GMP as well as [*rac*-**Me$_4$DAB**Pt(9-EtG)$_2$]$^{2+}$, no cross-peaks between the two (unequal) **G** H8 signals were observed, confirming the HT conformations. Our data demonstrate that no **Me$_4$DAB**Pt**G**$_2$ adduct formed an HH conformer as either a kinetic or a thermodynamic product, even when **G** = 5′-GMP (the **G** most favoring the HH conformer). Thus, the 5′-phosphate effect (which increases the abundance of the HH conformer in most other cases) could not overcome the strong steric effect of the **Me$_4$DAB** ligand in favoring the HT conformers. This absence of the HH conformer agrees with results reported for the [**Me$_4$EN**Pt(Guo)$_2$]$^{2+}$[31] and **Me$_4$DACH**Pt**G**$_2$ adducts.[53]

In contrast to **Me$_4$EN**Pt**G**$_2$ adducts, the absolute conformation (ΔHT or ΛHT) of the HT conformer of **Me$_4$DAB**Pt**G**$_2$ adducts can be assessed from NOE cross-peaks by exploiting the known absolute configuration of the chiral **Me$_4$DAB** carrier ligand. Furthermore, enhanced CD signals observed previously for *cis*-Pt**A**$_2$**G**$_2$ adducts have clear characteristics and can be utilized to identify the dominant HT conformer as ΔHT or ΛHT.[30,33,34,36,37,42,49−51] For all **Me$_4$DAB**Pt**G**$_2$ adducts, the CD signals have features similar to those found for previously studied *cis*-Pt**A**$_2$**G**$_2$ HT conformers.[30,33,34,36,37,42,49−51] Such similarity leads us to conclude that the CD features are similar for a particular conformer and reflective of the dominant conformer in solution, regardless of the identity of the carrier ligand, even when the ligand is as bulky as **Me$_4$DAB**.

Interligand Interaction Terms and Concepts for *cis*-PtA_2G_2 Adducts. We attribute the dominance of HT conformers over the HH conformer in both solution and the solid state to the more favorable dipole(base)−dipole(base) interaction and the lower base−base steric clashes of the HT versus HH orientation of bases relative to each other.[30,33−37,42,49,50] Because such interactions involve those parts of ligands close to the metal, we call these interligand interactions "first−to−first sphere communication" (FFC).[12,52] The favored HT conformer in *cis*-Pt**A**$_2$**G**$_2$ models with **G** = 5′-GMP can possibly be stabilized by carrier-ligand NH−5′-phosphate group hydrogen bonding; we call this interligand interaction "first−to−second sphere communication" (FSC) because a close-in ligand group (NH) is interacting with a peripheral group (5′-phosphate) in another ligand.[12,52]

Previously we demonstrated that, in the aqueous environment where the electrostatic attraction of the phosphate group to the cationic Pt moiety is weak, phosphate−*cis* **G** N1H interactions are a key factor in stabilizing the

(54) Booth, H.; Everett, J. R.; Fleming, R. A. *Org. Magn. Reson.* **1979**, *12*, 63–66.
(55) Miller, S. K.; Marzilli, L. G. *Inorg. Chem.* **1985**, *24*, 2421–2425.

favored HT conformer, especially for 5′-GMP.[34,36,42,51] We call such interligand interactions "second−to−second sphere communication" (SSC) because both interacting groups are at the periphery.[30,33,34,36,37,42] This specific favorable SSC interaction occurs when the guanine N1 remains protonated. Near pH 7, at which the phosphate group is deprotonated and dianionic, H-bonding can be enhanced but repulsions between the phosphate groups of adjacent GMP's also increase. This unfavorable repulsive SSC between two negative phosphate groups is also present at low pH. Nevertheless, in *cis*-PtA_2G_2 models, SSC interactions appear to have a net stabilizing effect on the ΛHT conformer in 5′-GMP adducts and on the ΔHT conformer in 3′-GMP adducts.[12,30,33,34,36,37,42,51,52,56]

Base Canting. In addition to the relative orientation of the five- and the six-membered rings, the bases in the conformers also cant (Figure 11), as shown by extensive NMR evidence.[30,33,34,36,37,42,49−51] Before discussing canting in the previous models and in **Me$_4$DAB**Pt**G**$_2$ adducts, we discuss relevant parameters found in X-ray structures of **Me$_4$EN**Pt**G**$_2$[20,57] and **Me$_4$DACH**Pt**G**$_2$ adducts.[58] For these structures, the N7−Pt−N−CH_3 torsion angle has a value of ∼70−80° for quasi-axial and 43−52° for quasi-equatorial N−Me groups in bidentate puckered N−C−C−N−Pt chelate rings. We use the C5−N7−Pt−*cis*-N torsion angle as a measure of base canting. When there is no canting, this angle has an absolute value of ∼90°. When the canting is away from the *cis*-N ('6-in', Figure 11), the value is greater than 90°. In the X-ray structures reported for **Me$_4$EN**Pt**G**$_2$ adducts with **G** = 9-methyl guanine (9-MeG) or 9-EtG,[20] one **G** base is not canted (C5−N7−Pt−*cis*-N torsion angle absolute value of ∼90°), while the other **G** base is canted away ('6-in') from the quasi-equatorial N-Me group (C5−N7−Pt−*cis*-N torsion angle has an absolute value of ∼95−98°). These values indicate that canting is minimal for both **G**'s. However, base canting is slightly larger (∼110°) for the ΛHT conformer of the **Me$_4$EN**Pt(5′-GMP)$_2$ adduct[57] and varied (99° to 108°) for the ΔHT conformers of the (*R*,*R*)- and (*S*,*S*)-**Me$_4$EN**Pt(5′-GMP)$_2$ adducts.[58]

Me$_2$DAB Pt**G**$_2$ adducts are particularly relevant to our discussion because in the common C_2-symmetrical configurations of the **Me$_2$DAB** ligand both N-Me groups are quasi-equatorial. Thus, these N-Me groups occupy roughly the same position as the quasi-equatorial **Me$_4$DAB** N-Me groups, one of the two types of **Me$_4$DAB** N-Me groups. In the major HT conformer of these **Me$_2$DAB**Pt**G**$_2$ adducts,[33−35] each guanine base has **G** O6 on the same side of the coordination plane as the cis quasi-equatorial N-Me group (Figure 11), and each base is canted away from the N-Me group so as to increase the **G** O6 to N-Me distance and avoid steric repulsion. The major form is '6-in'. (Note that the structures of the **Me$_4$EN**Pt**G**$_2$ adducts with **G** = 9-MeG or 9-EtG[20] are consistent with our interpretation of the results in **Me$_2$DAB**Pt**G**$_2$ adducts). The *S*,*R*,*R*,*S* chirality favors

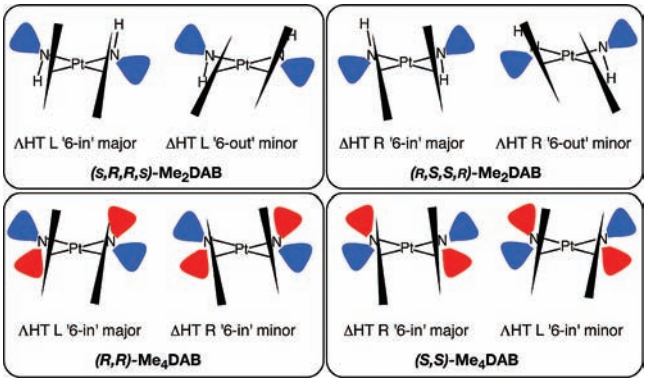

Figure 11. (Top): Sketches of the HT conformers of (*S*,*R*,*R*,*S*) and (*R*,*S*,*S*,*R*)-**Me$_2$DAB**Pt**G**$_2$ with left- and right-handed canting, respectively. (Bottom): Schematic representation of base orientations for the **Me$_4$DAB**Pt**G**$_2$ ΔHT and ΛHT forms. (**G** bases are shown as black triangles with five- and six-membered rings at tip and base, respectively. Blue (equatorial) and red (axial) areas represent out-of-plane bulk for the carrier ligand). Note that for **Me$_4$DAB**Pt**G**$_2$ the ΔHT form is '6-in' R and the ΛHT form is '6-in' L and that the '6-out' forms found in **Me$_2$DAB**Pt**G**$_2$ adducts are missing.

L canting, and the *R*,*S*,*S*,*R* chirality favors R canting (Figure 11).[29,30,33,34,36] This influence of the carrier ligand on canting has been found for adducts of all **G** derivatives and dinucleotides studied so far.[29,30,33,34,36] Because these interactions involve parts of ligands close to the metal, these are examples of FFC. In the major HT conformer, **G** O6 is located on the opposite side of the coordination plane from the carrier-ligand NH,[33,34,36] indicating that carrier-ligand H-bonding to **G** O6 is weak.[23,27,28,34,36] In the minor HT conformer of such **Me$_2$DAB**Pt**G**$_2$ adducts, the **G** O6 is on the same side of the coordination plane as the cis carrier-ligand NH. Furthermore, for a given chirality of the **Me$_2$DAB** ligand, the direction of canting is the *same* in both the major and the minor HT conformer of **Me$_2$DAB**Pt**G**$_2$ adducts (top of Figure 11).

Factors Influencing Canting and Stability. Relative to the case in which the bases are both perpendicular to the coordination plane, canting will move the six-membered rings closer to the midpoint between the N7 atoms ('6-in' form) or farther out from this midpoint ('6-out' form) (Figure 11). The consequences of L and of R canting are different for ΔHT and ΛHT conformers.[34] In each (*S*,*R*,*R*,*S*)-**Me$_2$DAB**Pt**G**$_2$ adduct, the canting is L, and for pH < 8, we find that the '6-in' major form is ΛHT L and the '6-out' minor form is ΔHT L. In each (*R*,*S*,*S*,*R*)-**Me$_2$DAB**Pt**G**$_2$ adduct, the canting is R, and for pH < 8, we find that the '6-in' major form is ΔHT R and the '6-out' minor form is ΛHT R.

The greater stability of the major '6-in' HT form of the **Me$_2$DAB**Pt**G**$_2$ adducts can reasonably be attributed to a preferred dipole interaction between the bases because having the larger six-membered guanine rings close to each other, as in the '6-in' form, is not a sterically favorable situation. Also, the **G** O6 favors the crowded side of the carrier ligand, and then the **G** base cants to minimize interactions. A striking example of the preference of **G** O6 for being close to N-Me groups is provided by adducts with the tridentate *N*,*N*′,*N*″-trimethyldiethylenetriamine ligand, **Me$_3$dien**Pt**G**,[59] in which two quasi-equatorial

(56) Williams, K. M.; Cerasino, L.; Intini, F. P.; Natile, G.; Marzilli, L. G. *Inorg. Chem.* **1998**, *37*, 5260–5268.
(57) Benedetti, M.; Tamasi, G.; Cini, R.; Marzilli, L. G.; Natile, G. *Chem.—Eur. J.* **2007**, *13*, 3131–3142.
(58) Benedetti, M.; Tamasi, G.; Cini, R.; Natile, G. *Chem.—Eur. J.* **2003**, *9*, 6122–6132.
(59) Carlone, M.; Fanizzi, F. P.; Intini, F. P.; Margiotta, N.; Marzilli, L. G.; Natile, G. *Inorg. Chem.* **2000**, *39*, 634–641.

N-Me groups are on the same side of the coordination plane. For **G** with no phosphate group, the rotamer with the **G** O6 near the more crowded region of the N-Me groups is the preferred rotamer by about 2:1 over the other rotamer.[59]

In minor '6-out' **Me$_2$DAB**Pt**G**$_2$ HT forms, **G** O6 is closer to the sterically less demanding NH part of **Me$_2$DAB** ligand, possibly allowing **G** O6−NH hydrogen bonding. Also, the bulkier six-membered rings are far from each other. These favorable FFC effects do not fully compensate for the FFC dipole effects, which appear to be less favorable in the '6-out' minor HT form, when compared to the '6-in' major HT form. As implied above, the minor conformer of (*S*,*R*,*R*,*S*)- and (*R*,*S*,*S*,*R*)-**Me$_2$DAB**Pt**G**$_2$ adducts could change its canting direction, becoming '6-in.' In the minor HT form, steric effects between the **G** O6's and the now-remote quasi-equatorial N-Me groups would not hinder this change in canting direction. Also, the steric interactions between the *cis* **G**'s would be compensated for by the dipole effects favoring '6-in' forms. Therefore, the reason that the minor form does not adopt this canting direction most probably lies in solvation effects. In a minor '6-in' HT form (not observed), the canting direction would place the **G** H8's closer to the N-Me group, a situation shown to be less common in the adducts with only one **G**.[60] The H8 is too far from the N-Me to have a direct steric interaction unless the base is highly canted. The H8 has a partial positive charge, as discussed for **G** and other lopsided ligands in a review.[61] In the '6-in' form the H8 atom is near the hydrophobic N-Me group; this position would be unfavorable because the solvation of the partially charged H8 would be decreased. Furthermore, in the minor HT conformer, the **G** O6's are on the side of the coordination plane near the NH's. Although **G** O6−NH H-bonding is weak, it will favor the '6-out' canting direction. Hence, the '6-in' canting direction is not observed in the minor HT conformer of **Me$_2$DAB**Pt**G**$_2$ adducts.

Base-Canting Effects on H8 Shifts in HT Conformers. The shift of the **G** H8 signal is generally useful for assessing the degree of base canting in all conformers.[12,30,33,34,36,38,40,62] The H8 signal experiences an upfield shift because of the ring-current anisotropy of the *cis* **G** base.[62] As an example, we describe the relationship of the **G** H8 shift to base canting for **Me$_2$DAB**Pt**G**$_2$. For **Me$_2$DAB**Pt**G**$_2$ adducts, the H8 signal of the major HT '6-in' form was always more downfield (typically by ∼0.25 ppm) than that of the minor '6-out' HT form.[34,36] This relationship suggested that the **G** bases in the minor form are canted '6-out', and therefore, each **G** has H8 toward the other **G**.

Base Canting in Me$_4$DABPtG$_2$ Adducts. H8 shifts may be used to assess canting. We initiate the discussion of H8 shifts with 9-EtG and 1-MeGuo adducts; these adducts do not have the complications caused by phosphate groups. Phosphate groups influence H8 shifts both directly by phosphate through-space anisotropic effects[34] and indirectly by effects of phosphate group H-bonding on canting.[49,50] The 8.21 and 8.22 ppm H8 shift values for the HT conformers of the [**Me$_4$DAB**Pt(9-EtG)$_2$]$^{2+}$ adduct are very similar and are closer to the 8.22 ppm shift of the major '6-in' HT form than to the 7.96 ppm value of the minor '6-out' HT form of the [**Me$_2$DAB**Pt(9-EtG)$_2$]$^{2+}$ adduct. The shifts for the latter differ. This comparison clearly indicates that both HT conformers of the [**Me$_4$DAB**Pt(9-EtG)$_2$]$^{2+}$ adduct have the '6-in' form (Figure 11). The main implication here is that the canting direction changes between the minor and major HT conformers so as to maintain the '6-in' base HT arrangement; this arrangement has favorable dipole−dipole interactions, while minimizing **G** O6 to **G** O6 and **G** O6 to N-Me steric clashes. Exactly the same reasoning and conclusion can be drawn from examining shift data for 1-MeGuo adducts, after allowing for the fact that the sugar causes the 1-MeGuo H8 signal to be ∼0.15 ppm downfield relative to the 9-EtG H8 signal. 1-MeGuo adducts have the following H8 shifts (ppm): **Me$_2$DAB**, 8.38 (major) and 8.14 (minor); and **Me$_4$DAB**, 8.41 to 8.44 (four forms), see Table 1. *These data provide the first clear example of a change in the canting direction between the two HT conformers of a cis-PtA$_2$**G**$_2$ adduct.*

The situation is rather complicated in cases for which SSC could have an effect. Nevertheless, the conclusions in the previous paragraph are supported by the similar H8 shifts of the major HT conformer (**G** O6 located on the same side of the coordination plane as the quasi-equatorial N-Me group) for **Me$_2$DAB**Pt**G**$_2$ and **Me$_4$DAB**Pt**G**$_2$ adducts, providing that the chelating carbons of these carrier ligands have the same chirality. For example, the similar H8 shifts of the major ΛHT conformer of (*S*,*R*,*R*,*S*)-**Me$_2$DAB**Pt(3′-GMP)$_2$ and (*R*,*R*)-**Me$_4$DAB**Pt(3′-GMP)$_2$ adducts[34] strongly indicate that the bases in these two major ΛHT conformers have similar spatial relationships relative to each other and to the coordination plane. Thus, the net steric effect of the equatorial N-Me groups is similar for the **Me$_2$DAB**Pt**G**$_2$ and **Me$_4$DAB**Pt**G**$_2$ adducts. The shifts of the signals of these N-Me groups (Supporting Information) are consistent with the orientation of the **G** base.

ΔHT:ΛHT Ratio. 9-EtG, Guo, and 1-MeGuo Adducts. The absence of NH groups in the **Me$_4$DAB** ligand eliminates FSC (carrier-ligand NH interaction with the phosphate group) as a factor influencing **Me$_4$DAB**Pt(GMP)$_2$ conformer distribution. To dissect the relative importance of FFC and SSC on the ΔHT:ΛHT ratio at equilibrium for **Me$_4$DAB**Pt(GMP)$_2$ adducts, we first discuss adducts with **G** derivatives (9-EtG, Guo, and 1-MeGuo) lacking a phosphate group and not influenced by SSC.

For [(*R*,*R*)-**Me$_4$DAB**Pt(Guo)$_2$]$^{2+}$ and [(*R*,*R*)-**Me$_4$DAB**Pt(1-MeGuo)$_2$]$^{2+}$, the ΛHT:ΔHT ratio was 2:1 (Table 2). Furthermore, the ΔHT:ΛHT ratio was 2:1 for the [(*S*,*S*)-**Me$_4$DAB**Pt(Guo)$_2$]$^{2+}$ and [(*S*,*S*)-**Me$_4$DAB**Pt(1-MeGuo)$_2$]$^{2+}$ adducts. Clearly, the chirality of the **Me$_4$DAB** ligand is the only factor that favors a particular HT chirality: *R*,*R* and *S*,*S* chiralities favor the ΛHT and ΔHT conformations, respectively. This information allows us to assign with complete confidence the HTa and HTb H8 signals for [*rac*-**Me$_4$DAB**Pt(9-EtG)$_2$]$^{2+}$ at equilibrium at pH 7 and 25 °C. The smaller HTa signal arises from the ΔHT [(*R*,*R*)-**Me$_4$DAB**Pt(9-EtG)$_2$]$^{2+}$ and ΛHT [(*S*,*S*)-**Me$_4$DAB**Pt(9-EtG)$_2$]$^{2+}$

(60) Carlone, M.; Marzilli, L. G.; Natile, G. *Inorg. Chem.* **2004**, *43*, 584–592.
(61) Marzilli, L. G.; Marzilli, P. A.; Alessio, E. *Pure Appl. Chem.* **1998**, *70*, 961–968.
(62) Kozelka, J.; Fouchet, M. H.; Chottard, J.-C. *Eur. J. Biochem.* **1992**, *205*, 895–906.

pair and the larger HTb signal from the ΛHT [(*R*,*R*)-**Me$_4$DAB**Pt(9-EtG)$_2$]$^{2+}$ and ΔHT [(*S*,*S*)-**Me$_4$DAB**Pt(9-EtG)$_2$]$^{2+}$ pair (Tables 1 and 2).

The reasons for the observed ratios are clear. Because **G** O6 clashes with the *cis*-N-Me groups would be severe in the '6-out' arrangement, this arrangement is unfavorable and both HT conformers are '6-in.' The HT conformer with a quasi-equatorial N-Me and a *cis*-**G** H8 on the same side of the coordination plane is less favorable than the HT conformer with a quasi-axial N-Me and a *cis*-**G** H8 on the same side of this plane. Because the '6-in' HT conformers have long distances between the **G** O6 and *cis*-N-Me groups, this difference in stability may be caused by differences in the strength of the clash between N-Me and *cis*-**G** H8 groups. This clash appears to be greater for the quasi-equatorial N-Me group than for the quasi-axial N-Me group because the *cis*-**G** H8 protrudes more toward the quasi-equatorial N-Me group. Also, unlike the case in which there are NH groups on the carrier ligand, the canting direction changes. Both HT forms are '6-in.' The H8 shifts, as mentioned above, are consistent with this analysis.

HT Ratio for Me$_4$DABPt(5′-GMP)$_2$ Adducts. For (*R*,*R*)-**Me$_4$DAB**Pt(5′-GMP)$_2$, the *R*,*R* carrier-ligand chirality (FFC) and the 5′-phosphate group to *cis*-**G** H-bonding (SSC) both favor the ΛHT conformation. As a result, the ΛHT:ΔHT ratio of 6:1 at pH 7.3 (Table 2) was higher than the 2:1 value for adducts such as 9-EtG (with no SSC). Although the ratio of ∼4:1 for (*R*,*R*)-**Me$_4$DAB**Pt(5′-GMP)$_2$ at pH 4.1 was lower, it clearly indicates that the 5′-phosphate group has an SSC effect even at pH 4.1.

The (*S*,*S*)-**Me$_4$DAB**Pt(5′-GMP)$_2$ adduct at pH 4.0 has a very weak CD signal (Supporting Information) and ΛHT and ΔHT conformers in roughly equal abundance (Figure 7). The ΔHT:ΛHT ratio of ∼1 reflects the counteracting effects of FFC (*S*,*S* chirality of the **Me$_4$DAB** ligand favoring the ΔHT conformer) and SSC (5′-GMP favoring the ΛHT conformer). Furthermore, the abundance of the ΛHT conformer increased from pH 4.0 to pH 7.4, confirming the importance of SSC.

The results for the GMP adducts clearly demonstrate that SSC is stronger for 5′-GMP than for 3′-GMP adducts at pH ∼4, where the phosphate group is protonated. The HT conformer with the chirality favored by SSC increased from pH ∼4 to ∼7 in all cases, confirming that a deprotonated phosphate group has a greater SSC effect than a protonated phosphate group.

HT Ratio for Me$_4$DABPt(3′-GMP)$_2$ Adducts. For (*S*,*S*)-**Me$_4$DAB**Pt(3′-GMP)$_2$, the ΔHT conformer is favored by both the chirality of the **Me$_4$DAB** ligand (FFC) and the mutual 3′-PO$_4$−N1H interactions of the 3′-GMP's (SSC). For (*R*,*R*)-**Me$_4$DAB**Pt(3′-GMP)$_2$, the ΛHT conformer is favored by FFC, whereas SSC involving 3′-GMP continues to favor the ΔHT conformer. However, for both 3′-GMP adducts at pH ∼4.0 (Table 2), the results are similar to those found for **G** derivatives lacking a phosphate group and for which FFC dominates. Thus, SSC is negligible for 3′-GMP adducts at low pH, where the 3′-phosphate is protonated. In contrast, for both adducts at pH ∼7.0, SSC clearly becomes important, and the ΔHT conformer becomes more favored. In addition, the H8 signal of the ΔHT conformer of both adducts shifted downfield (Table 1), consistent with a greater degree of canting caused by the SSC interaction. This relationship was noted previously.[30,36] The H8 signal of the ΛHT conformer of both adducts did not shift. These observations all indicate that the interaction of the 3′-phosphate group with the NH group of the *cis*-3′-GMP is more favorable in the ΔHT conformer than in the ΛHT conformer.

Influence of N1H Deprotonation on the Me$_4$DABPtG$_2$ Adducts. To understand the effects of N1H deprotonation, we first consider past studies with 9-EtG adducts because there are no complicating effects of SSC or FSC involving the phosphate group. Only FFC is important in 9-EtG adducts. Studies at high pH are complicated by isomerization of the asymmetric HNMe groups in **Me$_2$DAB**PtG$_2$ adducts at high pH, especially problematic for cationic adducts, such as [**Me$_2$DAB**Pt(9-EtG)$_2$]$^{2+}$. Consequently, some years ago we began to study **Bip**PtG$_2$ analogues, which generally mimic the conformational behavior of **Me$_2$DAB**PtG$_2$ adducts but which have configurations at the **Bip** NH's resistant to isomerization.[27,34] Therefore, effects of N1H deprotonation at high pH upon the [**Me$_4$DAB**Pt(9-EtG)$_2$]$^{2+}$ adduct will thus be compared to those for the [**Bip**Pt(9-EtG)$_2$]$^{2+}$ adduct.[30]

The ratio, '6-in' HT:'6-out' HT, inverted from >1 to <1 upon N1H deprotonation of the [**Bip**Pt(9-EtG)$_2$]$^{2+}$ adduct.[30] Note that the two HT conformers have different chirality, as shown for **Me$_2$DAB**PtG$_2$ adducts in Figure 11. The increase in stability of the '6-out' HT conformer relative to the '6-in' HT conformer can arise from two causes: (i) a reduction of electrostatic repulsion between the two negatively charged N1 atoms, which in a '6-out' HT conformer is placed farther apart than in the '6-in' HT conformer; and (ii) an enhancement of the **G** O6−(NH)**Bip** H-bonding as a result of the increase in H-bond acceptor capacity of the now more electron-rich **G** O6.[34,36] In the '6-out' HT conformer, the **G** O6 is positioned to form such an H-bond. The second cause is absent in the [**Me$_4$DAB**Pt(9-EtG)$_2$]$^{2+}$ adduct. (A highly canted '6-out' HT conformer is not possible for steric reasons, and no NH in the carrier ligand is present to form an H-bond.) The major HT:minor HT ratio of the [**Me$_4$DAB**Pt-(9-EtG)$_2$]$^{2+}$ adduct is insensitive to deprotonation, in marked contrast to the behavior of the [**Bip**Pt(9-EtG)$_2$]$^{2+}$ adduct. Thus, FFC involving the **G** O6 to N-Me steric effects outweighs other factors influencing the ratio of HT conformers.

In studies of *cis*-PtA$_2$(GMP)$_2$ adducts,[30,34,37] changes caused in the major HT:minor HT ratio by N1H deprotonation are more difficult to interpret than for adducts with **G**'s lacking a phosphate group. The phosphate group can have unfavorable repulsive interactions with the N1$^-$ groups. This unfavorable SSC is most severe when the HT chirality places the phosphate group close to N1 (as when the HT chirality is favored by phosphate−N1H H-bonding at pH 7). Thus, phosphate−N1$^-$ repulsion is greatest for 5′-GMP adducts when the HT chirality is Λ and for 3′-GMP adducts when the HT chirality is Δ. For 5′-GMP adducts having NH-bearing carrier ligands, the potential involvement of this NH in an H-bond with the phosphate group (a FSC interaction) further complicates the interpretation of the high pH data. This difficulty plagues the analysis of 5′-GMP adducts of cisplatin and of even less dynamic adducts, making it difficult to explain all the high-pH results.[30,34,37,51]

The ratio, major '6-in' HT:minor '6-in' HT, changed dramatically for the **Me$_4$DAB**Pt(5′-GMP)$_2$ and **Me$_4$DAB**Pt-(3′-GMP)$_2$ complexes upon N1H deprotonation (Table 2).

Such behavior is expected if phosphate−N1$^-$ repulsion is important. The pH ∼10 data in Table 2 can be understood as resulting from the interplay of two factors, **Me$_4$DAB** chirality (FFC) and phosphate−N1$^-$ repulsion (SSC). We use (*R*,*R*)-**Me$_4$DAB**Pt(GMP)$_2$ adducts to illustrate this interplay. When the GMP is 3′-GMP, the two factors work in concert and both favor the ΛHT conformer; consequently, a highly abundant ΛHT conformer was found (∼80%). When GMP is 5′-GMP, the two factors oppose each other. FFC favors the ΛHT conformer, and SSC repulsion involving N1$^-$ favors the ΔHT conformer; accordingly, the two HT conformers have similar abundance (Table 2). The (*R*,*R*)-**Me$_4$DAB**Pt(GMP)$_2$ results exhibit a satisfying symmetry with the (*S*,*S*)-**Me$_4$DAB**Pt-(GMP)$_2$ results. When both factors work in concert (now favoring the ΔHT conformer), as in the (*S*,*S*)-**Me$_4$DAB**Pt-(5′-GMP)$_2$ case, the conformer in 80% abundance at pH 10 is ΔHT, as expected. Such complementary relationships are absent in previous studies because of the presence of FSC effects and of both '6-in' and '6-out' HT conformers.[30,34] As a result, a very high percentage of one conformer was not found previously under these conditions.

Conclusions

Even in the case of **G** = 5′-GMP, a nucleotide known to enhance the stability of the HH conformer, we found no head-to-head (HH) conformer for the **Me$_4$DAB**Pt**G$_2$** adducts. A significant advantage in investigating the **Me$_4$DAB**Pt**G$_2$** complexes over the **Me$_4$EN**Pt**G**$_2$ adducts, which were used in the now-classical seminal study of HT conformers exhibiting slow interchange,[31] is the utility of the **Me$_4$DAB** ligand for determining the absolute conformation of the HT conformers. We were also able to define the canting direction by comparison to results with **Me$_2$DAB**Pt**G$_2$** adducts, where canting is well defined.[33,34] We conclude that in the **Me$_4$DAB**Pt**G$_2$** HT conformers the bases cant slightly in such a direction as to avoid the clashes between the **Me$_4$DAB** N-Me groups and **G** O6's. This canting produces '6-in' conformers with more favorable dipole(base)−dipole(base) interactions than the '6-out' conformers. As a result, in contrast to previous cases, we have clear evidence that the direction of canting changes as the ΔHT and ΛHT conformers interconvert.

For **Me$_4$DAB**Pt**G$_2$** adducts, the canting degree that is optimal for favorable base−base interactions in the '6-in' conformer creates a relatively long distance between **G** O6 and the N-Me group. The estimated ∼3.6 Å distance is too large for steric factors to control the canting degree. Nevertheless, the **Me$_4$DAB** chirality does influence the relative stability of the ΔHT and ΛHT conformers. The HT conformer with a quasi-equatorial N-Me and a *cis*-**G** H8 on the same side of the coordination plane is less favorable than the HT conformer with a quasi-axial N-Me and a *cis*-**G** H8 on the same side of this plane. Because the '6-in' HT conformers have long distances between the **G** O6 the *cis*-N-Me groups, this difference in stability may be caused by differences in the strength of the clash between N-Me and *cis*-**G** H8 groups. This clash appears to be greater for the quasi-equatorial N-Me group than for the quasi-axial N-Me group because the *cis*-**G** H8 protrudes more toward the quasi-equatorial N-Me group.

In GMP adducts, FFC, SSC, and (sometimes) FSC are possible. Only SSC and FFC interactions are relevant for **Me$_4$DAB**Pt**G$_2$** adducts. The dependence of the ΔHT:ΛHT ratio for all **Me$_4$DAB**Pt(GMP)$_2$ adducts on pH changes from ∼4 to ∼7 is consistent with previously identified factors that influence this ratio. Our results show that SSC has more general relevance because it is important when both HT conformers are '6-in' as well as when one is '6-in' and the other is '6-out.'

The effects of changes in solution pH from ∼7 to ∼10 on the ΔHT:ΛHT ratio are more easily understood for all **Me$_4$DAB**Pt**G$_2$** adducts than for previously studied slowly interconverting *cis*-A$_2$Pt**G**$_2$ HT conformers. No inversion in abundance of the HT conformers of [**Me$_4$DAB**Pt(9-EtG)$_2$]$^{2+}$ occurred when the pH was raised from ∼7 to ∼10. For previously studied adducts, the ratio inverted in most cases to favor the '6-out' conformer.[34] Release of N$^-$−N$^-$ electrostatic repulsion can occur by an increase in canting of the '6-out' conformer; the carrier ligands used in previous studies offered ample space to accommodate the canting because they are less bulky than **Me$_4$DAB**.

The abundance of the HT conformers of **Me$_4$DAB**Pt-(GMP)$_2$ adducts changed when the pH was raised from ∼7 to ∼10. These changes can be understood in terms of unfavorable SSC repulsive effects, which decrease the stability of just those forms favored by attractive favorable SSC effects at pH ∼7. Those conformers in which the phosphate−N1H H-bonding is favorable at pH ∼7 are exactly the conformers in which this proximity becomes repulsive when the N1H is deprotonated. For previous models, this same relationship plays a role, but the results are not so clearly understood because FFC is not restricted to interligand clashes, as is the case for **Me$_4$DAB**Pt(GMP)$_2$ adducts. In addition, previous adducts also underwent changes in canting when the N1H was deprotonated.[34]

Our study of **Me$_4$DAB**Pt**G$_2$** adducts has thus both reinforced conclusions from our earlier work and provided new information not previously revealed in studies with less bulky ligands or with ligands lacking chiral centers. In unpublished work in preparation, we find that the HH conformer is less favored in **Me$_4$DAB**Pt(dGpG) and **Me$_4$DAB**Pt(oligo) than in other cross-link adducts, even though the phosphodiester backbone link in G*pG* adducts normally favors the HH conformation associated with the lesion believed to be responsible for activity. Thus, future studies with **Me$_4$DAB**Pt adducts may provide additional new insights into the functional role of the carrier ligand in influencing the nature of Pt−DNA adducts and hence anticancer activity.

Acknowledgment. This work was supported by the University of Bari and the EC (COST Action D39) to G.N. and the UAB Comprehensive Cancer Center to J.S.

Supporting Information Available: A detailed description for synthesizing **Me$_4$DAB**Pt(NO$_3$)$_2$ complexes; assignment methods for conformers; tables of chemical shifts and relative volumes for various cross-peaks of **Me$_4$DAB**Pt**G$_2$** adducts; ^{1}H NMR spectra for free (*R*,*R*)- and [(*S*,*S*)-**Me$_4$DAB**Pt(D$_2$O)$_2$]$^{2+}$ complexes; NOESY and HMQC spectra for (*R*,*R*)- and (*S*,*S*)-**Me$_4$DAB**Pt(3′-GMP)$_2$; conformer distribution versus time for various adducts; ^{1}H NMR and CD spectra of various **Me$_4$DAB**Pt**G$_2$** adducts recorded at various pH values. This material is available free of charge via the Internet at http://pubs.acs.org.